



**HAL**  
open science

## Green emitting $\beta$ -SiAlON:Eu<sup>2+</sup> phosphors derived from chemically modified perhydropolysilazanes

Yang Gao, Ryo Iwasaki, Daiki Hamana, Junya Iihama, Sawao Honda, Munni Kumari, Tomokatsu Hayakawa, Samuel Bernard, Philippe Thomas, Yuji Iwamoto

### ► To cite this version:

Yang Gao, Ryo Iwasaki, Daiki Hamana, Junya Iihama, Sawao Honda, et al.. Green emitting  $\beta$ -SiAlON:Eu<sup>2+</sup> phosphors derived from chemically modified perhydropolysilazanes. International Journal of Applied Ceramic Technology, 2022, 10.1111/ijac.14139 . hal-03851852

**HAL Id: hal-03851852**

**<https://cnrs.hal.science/hal-03851852v1>**

Submitted on 14 Nov 2022

**HAL** is a multi-disciplinary open access archive for the deposit and dissemination of scientific research documents, whether they are published or not. The documents may come from teaching and research institutions in France or abroad, or from public or private research centers.

L'archive ouverte pluridisciplinaire **HAL**, est destinée au dépôt et à la diffusion de documents scientifiques de niveau recherche, publiés ou non, émanant des établissements d'enseignement et de recherche français ou étrangers, des laboratoires publics ou privés.

# Green emitting $\beta$ -SiAlON:Eu<sup>2+</sup> phosphors derived from chemically modified perhydropolysilazanes

Yang Gao<sup>1</sup> | Ryo Iwasaki<sup>1</sup> | Daiki Hamana<sup>1</sup> | Junya Iihama<sup>1</sup> | Sawao Honda<sup>1</sup>  |  
Munni Kumari<sup>2</sup> | Tomokatsu Hayakawa<sup>1</sup> | Samuel Bernard<sup>2</sup>  
Philippe Thomas<sup>2</sup> | Yuji Iwamoto<sup>1</sup> 

<sup>1</sup>Department of Life Science and Applied Chemistry, Graduate School of Engineering, Nagoya Institute of Technology, Showa-ku, Nagoya, Japan

<sup>2</sup>University of Limoges, CNRS, IRCER, Limoges, France

## Correspondence

Yuji Iwamoto, Department of Life Science and Applied Chemistry, Graduate School of Engineering, Nagoya Institute of Technology, Gokiso-cho, Showa-ku 466-8555, Nagoya, Japan.  
Email: iwamoto.yuji@nitech.ac.jp

## Funding information

Japan Science and Technology Agency, Grant/Award Number: JPMJSP 2112

## Abstract

We report the first synthesis of  $\beta$ -SiAlON:Eu<sup>2+</sup> phosphors from *single-source* precursors, perhydropolysilazane (PHPS), chemically modified with Al(OCH(CH<sub>3</sub>)<sub>2</sub>)<sub>3</sub>, and EuCl<sub>2</sub>. The reactions occurring during the precursor synthesis and the subsequent thermal conversion of polymeric precursors into  $\beta$ -SiAlON:Eu<sup>2+</sup> phosphors have been studied by a complementary set of analytical techniques, including infrared spectroscopy, gas chromatography–mass spectrometry, thermogravimetry–mass spectrometry, X-ray diffraction (XRD), photoluminescence spectroscopy, and scanning electron microscopy. It has been clearly established that Al(OCH(CH<sub>3</sub>)<sub>2</sub>)<sub>3</sub> immediately reacted with PHPS to afford N–Al bonds at room temperature, whereas N–Eu bond formation was suggested to proceed above 600°C accompanied by the elimination of HCl up to 1000°C in flowing N<sub>2</sub>. The subsequent 1800°C-heat treatment for 1 h under an N<sub>2</sub> gas pressure at 980 kPa allowed converting the *single-source* precursors into fine-grained  $\beta$ -SiAlON:Eu<sup>2+</sup> phosphors. XRD analysis revealed that the Al/Si of .09 was the critical atomic ratio in the precursor synthesis to afford single-phase  $\beta$ -SiAlON ( $z = .55$ ). Moreover, Eu<sup>2+</sup>-doping was found to efficiently reduce the carbon impurity in the host  $\beta$ -SiAlON. The polymer-derived  $\beta$ -SiAlON:Eu<sup>2+</sup> phosphors exhibited green emission under excitation at 460 nm and achieved the highest green emission intensity at the critical dopant Eu<sup>2+</sup> concentration at 1.48 at%.

## KEYWORDS

europium, oxynitride, photoluminescence, polymer precursor, SiAlON

## 1 | INTRODUCTION

Solid-state lighting (SSL) solution has been worldwide spread to replace the traditional illumination source, such as incandescent and fluorescent lamps, to save a huge amount of energy and reduce the carbon emission. Among the SSL sources, phosphors-converted white LEDs have attracted extensive attention because of their great

luminous efficiency, flexible color design, and relatively low cost.<sup>1</sup> Current high-quality white light has been developed by assembling the blue LED chips with green and red phosphors (two-pc-wLEDs). The green phosphors applied for the two-pc wLEDs are oxynitride phosphors based on Eu<sup>2+</sup>-activated  $\beta$ -SiAlON, which have been recently developed to be substituted for sulfide-based phosphors.

$\beta$ -SiAlON with the general formula  $\text{Si}_{6-z}\text{Al}_z\text{O}_z\text{N}_{8-z}$  ( $0 \leq z \leq 4.2$ ) is a solid solution of  $\beta$ -silicon nitride ( $\text{Si}_3\text{N}_4$ ) and aluminum oxide ( $\text{Al}_2\text{O}_3$ ) formed by partial replacement of Si–N bond with Al–O or Al–N bond, whereas  $\text{Eu}^{2+}$ -activated  $\beta$ -SiAlON can be expressed by the modified formula of  $\text{Si}_{6-z}\text{Al}_z\text{O}_{z-2y}\text{N}_{8-z+2y}:\text{yEu}^{2+}$ , which takes into account the charge compensation by  $\text{Eu}^{2+}$ -doping.<sup>2</sup> Photoluminescent (PL) properties of  $\text{Eu}^{2+}$ -activated  $\beta$ -SiAlON ( $\beta$ -SiAlON: $\text{Eu}^{2+}$ ) phosphors depend on several material factors, including  $z$  value,<sup>3</sup> amount of  $\text{Eu}^{3+}$  as killer site,<sup>4</sup> and morphology and the phase purity of host  $\beta$ -SiAlON.<sup>5</sup> Hirasaki et al. fabricated  $\beta$ -SiAlON: $\text{Eu}^{2+}$  phosphors with several  $z$  values and  $\text{Eu}^{2+}$  concentrations. They found that impurity SiAlON polytypoid phases, such as 12H, 21R, and 27R, appeared either by increasing  $z$  value or  $\text{Eu}^{2+}$  molar percentage.<sup>6</sup> Based on these results, they suggested that critical  $\text{Eu}^{2+}$  concentrations are  $\sim .7$  and  $.5$  at% for the host  $\beta$ -SiAlON with  $z = .1$  and  $.5$ , respectively, and  $\beta$ -SiAlON: $\text{Eu}^{2+}$  phosphors with  $z$  values ranging from  $.1$  to  $.5$  are suitable for practical applications.<sup>6</sup> Kikkawa et al. reported that the morphology of  $\beta$ -SiAlON ceramics changed from rod-like to near-equiaxed shape at the  $z$  value from 1.0 to 2.0, whereas the green emission color shifted to a lower wavelength consistently with the  $z$  value and finally turned to be blue at  $z = 4$ .<sup>5</sup>

$\beta$ -SiAlON ceramics can be fabricated by the conventional powder metallurgy method using starting powders of  $\alpha$ - $\text{Si}_3\text{N}_4$ ,  $\alpha$ - $\text{Al}_2\text{O}_3$  and aluminum nitride (AlN). Generally, fabrication conditions of high-temperature heat treatment at  $T \geq 1800^\circ\text{C}$  under a high nitrogen ( $\text{N}_2$ ) pressure at  $p \geq .98$  MPa are required to afford  $\beta$ -SiAlON as a thermodynamically favorable phase.<sup>3,6</sup>

On the other hand, a novel polymer-derived ceramics (PDCs) route has been found as convenient and appropriate for the synthesis of silicon (Si)-based non-oxide ceramic systems.<sup>7–10</sup> The PDCs route offers several potential advantages, including compositional homogeneity, purity, and structure tailorability, which can be achieved by an in situ formation of polycrystalline ceramics from a novel metastable amorphous compound produced by pyrolysis of a *single-source* precursor, in which strictly controlled chemical composition can be established at molecular scale.<sup>11–14</sup> In this route, perhydropolysilazane (PHPS) composed of only Si, N, and H has some advantages in high purity for the synthesis of  $\text{Si}_3\text{N}_4$  ceramics.<sup>8,9</sup> Moreover, PHPS can be easily modified with various organometallic compounds to afford *single-source* precursors containing appropriate elements for Si-based multicomponent non-oxide ceramic systems.<sup>15–24</sup> In Ref. [16], polyaluminosilazanes synthesized by chemical modification of PHPS with (ethyl acetoacetate) aluminum di(isopropoxide) have been successfully converted to appropriate quaternary Si–Al–O–N amorphous compound by pyrolysis at  $1000^\circ\text{C}$

under flowing ammonia ( $\text{NH}_3$ ). However, subsequent heat treatment up to  $1500^\circ\text{C}$  in  $\text{N}_2$  resulted in the partial crystallization of  $\beta$ -SiAlON or the formation of a mixture of  $\beta$ -SiAlON, J-SiAlON, and mullite ( $3\text{Al}_2\text{O}_3-2\text{SiO}_2$ ) phases due to the excess oxygen introduced from the Al alkoxide modifier.<sup>16</sup> On the other hand, polymers containing nanometer-sized filler particles, such as polycarbosilane combined with aluminum hydroxide ( $\text{Al}(\text{OH})_3$ ) nanoparticles derived from  $\text{Al}(\text{O-secBu})_3$ <sup>25</sup> and polysilazane mixed with nanofillers containing  $\text{Si}_3\text{N}_4$ – $\text{Al}_2\text{O}_3$ –AlN<sup>26</sup> or  $\text{Al}_2\text{O}_3$ ,<sup>27</sup> have been reported as useful for the formation of SiAlON-based ceramics. However, as far as we know, no research work has been dedicated to the accurate chemical composition and structure controlling at the nano- to micrometer scale of  $\beta$ -SiAlON: $\text{Eu}^{2+}$  phosphors through the PDCs route.

Herein, we conducted syntheses of a series of  $\beta$ -SiAlON: $\text{Eu}^{2+}$  phosphor samples through the PDCs route: *single-source* polymeric precursors, in which strictly controlled chemical composition is established at molecular scale have been synthesized by chemical modification of a commercially available PHPS ( $(\text{SiH}_2\text{-NH})_n$ ) with aluminum triisopropoxide ( $\text{Al}(\text{OCH}(\text{CH}_3)_2)_3$ ) and europium(II) chloride ( $\text{EuCl}_2$ ).

The *single-source* precursors are converted to  $\text{Eu}^{2+}$ -doped amorphous SiAlON by pyrolysis at  $1000^\circ\text{C}$  under flowing  $\text{N}_2$ . Subsequently, the polymer-derived multicomponent amorphous compounds are converted to  $\beta$ -SiAlON: $\text{Eu}^{2+}$  phosphors by heat treatment up to  $1800^\circ\text{C}$  under an  $\text{N}_2$  gas pressure at 980 kPa. The relationships between the chemical composition in terms of  $\text{Eu}^{2+}$  concentration, phase purity and morphology of host  $\beta$ -SiAlON, and PL properties of the polymer-derived  $\beta$ -SiAlON: $\text{Eu}^{2+}$  phosphor samples are discussed based on a set of characterization techniques, including infrared spectroscopy, gas chromatography–mass spectrometric (GC–MS) analyses, simultaneous thermogravimetric–MS (TG–MS) analyses, X-ray diffraction (XRD), PL spectroscopy, and scanning electron microscope (SEM) observations.

## 2 | EXPERIMENTAL PROCEDURES

### 2.1 | Materials and methods

Commercially available PHPS (99.993%, Si, 67.91; N, 27.77; H, 4.313 wt%, AZ NN110-20, 20-wt% xylene solution, AZ Electronic Materials Co., Ltd., Tokyo, Japan),  $\text{Al}(\text{OCH}(\text{CH}_3)_2)_3$  (99.9%, Kojundo Chemical Laboratory Co. Ltd., Saitama, Japan), and  $\text{EuCl}_2$  (99.9%, Sigma-Aldrich Japan, Tokyo, Japan) were used without further purification and handled under dry argon (Ar) atmosphere using standard Schlenk techniques.

As a typical experiment, we described the synthesis of Al, Eu-modified PHPS labeled as SAE95, and its conversion to  $\beta$ -SiAlON:Eu<sup>2+</sup> phosphor: a 300-ml two-neck round-bottom flask equipped with a magnetic stirrer was charged with 20-wt% xylene solution of PHPS (10 ml, hence Si = 1.36 g, 48.4 mmol), Al(OCH(CH<sub>3</sub>)<sub>2</sub>)<sub>3</sub> (.893 g, 4.37 mmol), and EuCl<sub>2</sub> (.542 g, 2.43 mmol) and then refluxed for 1 h. After the reaction mixture was cooled down to room temperature (RT), the solvent was removed under vacuum at RT to give SAE95 as white solid. Subsequently, the SAE95 sample was pyrolyzed by a tube furnace (model ARF60–150–31KC, Asahi Rika, Chiba, Japan) under flowing N<sub>2</sub> at 1000°C for 1 h with a heating rate of 5°C min<sup>-1</sup>. The pyrolyzed powder was converted to  $\beta$ -SiAlON:Eu<sup>2+</sup> phosphor by heat treatment in a graphite resistance-heated furnace (model High Multi 5000, Fujidempa Kogyo, Co., Ltd., Osaka, Japan) at 1800°C for 1 h under an N<sub>2</sub> gas pressure at 980 kPa.

## 2.2 | Characterizations

The chemical modification reactions of PHPS were monitored by attenuated total reflection Fourier transform infrared (ATR-FTIR) spectroscopy using a FTIR spectrometer (model FT/IR-4200IF, JASCO Corporation, Tokyo, Japan) attached with an ATR equipment (model ATR PRO 550S-S/570S-H, JASCO Corporation, Tokyo, Japan) at a resolution of 4 cm<sup>-1</sup>.

The details of the chemical reactions during the precursor synthesis from RT to 140°C (xylene reflux) and precursor pyrolysis up to 1000°C were monitored by GC–MS and TG–MS analyses under He flow, respectively (model STA7200, Hitachi, Tokyo, Japan). Commercially available isopropanol (≥99%, Sigma-Aldrich Japan, Tokyo, Japan) was used as a reference for the GC–MS analyses.

XRD analysis for the heat-treated samples was performed (model X' Pert-Pro  $\alpha$ 1, PANalytical, UK) using a Cu K $\alpha$  radiation.

The  $\beta$ -phase ratio of the polymer-derived SiAlON-based samples was defined as the  $\beta/(\beta + \alpha)$ -phase ratio evaluated by comparing the diffraction peak intensity ( $I$ ) of the  $\alpha$ -phase (102), (210) plane and  $\beta$ -phase (101), (210) plane<sup>28</sup>:

$$\beta - \text{phase ratio} = \frac{(I\beta(101) + I\beta(210))}{(I\beta(101) + I\beta(210)) + (I\alpha(102) + I\alpha(210))} \times 100 \quad (1)$$

Elemental analyses for oxygen (O), nitrogen (N) by the inert-gas fusion method (model EMGA-930, Horiba, Kyoto, Japan), and carbon (C) by the nondispersive infrared method (model CS844, LECO CORPORATION,

St. Joseph, USA) were performed on the 1000°C-pyrolyzed and subsequent 1800°C heat-treated samples. The Al and Eu contents in the polymer-derived SiAlON:Eu<sup>2+</sup> samples were analyzed by using an energy-dispersive X-ray spectrometer (EDS) mounted on an SEM (model JSM-6010LA, JEOL Ltd., Tokyo, Japan). In this study, EDS element mapping analysis was performed on the powdered sample surfaces observed within an SEM image area of  $\sim 20 \times 25 \mu\text{m}^2$  at the magnification and accelerating voltage of 5000x and 15 kV, respectively, to give an atomic percentage for all the constituent elements. For each sample, the Al/Si and Eu/Si ratios were evaluated as an average value of the mapping scans conducted for at least five different areas randomly selected. Then, the chemical composition of the polymer-derived SiAlON-based samples was determined as follows:

$$\text{wt\% (Si + Al + Eu)} = 100\% - \text{wt\% (C)} - \text{wt\% (N)} - \text{wt\%} \quad (2)$$

Morphology of the polymer-derived  $\beta$ -SiAlON:Eu<sup>2+</sup> samples was observed by using an SEM (model JSM-6010LA, JEOL Ltd., Tokyo, Japan).

The PL emission and excitation spectra were recorded at RT using a fluorescence spectrometer (model F-7000, Hitachi, Tokyo, Japan) with a xenon (Xe) lamp.

## 3 | RESULTS AND DISCUSSION

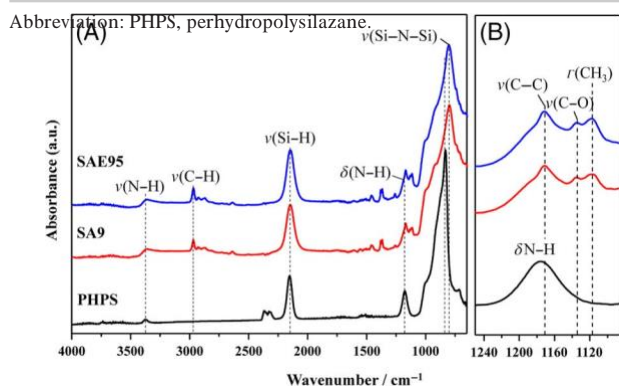
### 3.1 | Synthesis of *single-source* precursors and their conversion into inorganic compounds

*Single-source* precursor syntheses in this study were conducted for the compositions listed in Table 1. The nominal  $z$  value of the host  $\beta$ -SiAlON was calculated using the theoretical formula, Si<sub>6-z</sub>Al<sub>z</sub>O<sub>z-2y</sub>N<sub>8-z+2y</sub>:yEu<sup>2+</sup>, given by Wang et al.<sup>2</sup>

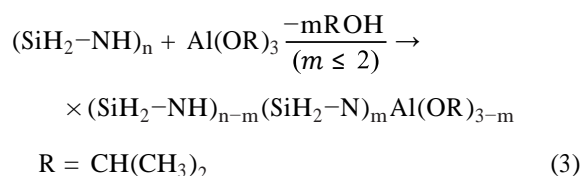
To clarify the necessary amount for an in situ formation of host  $\beta$ -SiAlON with  $z$  value  $\leq 5$ ,<sup>6</sup> the amount of the Al(OiPr)<sub>3</sub> was examined at the Al/Si ratios of .03, .06, and .09, and the resulting precursors were labeled as SA3, SA6, and SA9, respectively. On the other hand, to investigate the effect of the amount of Eu-doping on the formation and PL properties of the polymer-derived  $\beta$ -SiAlON:Eu<sup>2+</sup>, the amount of EuCl<sub>2</sub> for the chemical modification was examined at the Eu/Si atomic ratios of .01, .03, .05, and .07, and the synthesized precursors were labeled as SAE91, SAE93, SAE95, and SAE97, respectively. At the polymeric precursor state, the resulting anion contents, O and N need modified expression as Si<sub>6-z</sub>Al<sub>z</sub>O<sub>z-2y+\delta</sub>N<sub>8-z+2+\gamma</sub>:yEu<sup>2+</sup>. The value of differences,  $\delta$  and  $\gamma$  for each composition are also listed in this table.

**TABLE 1** Nominal molar ratios for synthesis of *single-source* precursors for  $\beta$ -SiAlON and  $\text{Eu}^{2+}$ -activated  $\beta$ -SiAlON phosphors

Name	Si in ( $\text{SiH}_2\text{-NH}$ ) <sub>n</sub> (PHPS)	M/Si ratio		Formula	Calculated chemical composition				$\text{Eu}^{2+}$ (at%)
		$\text{Al}(\text{OCH}(\text{CH}_3)_2)_3$	$\text{EuCl}_2$		$\text{Si}_{6-z}\text{Al}_z\text{O}_{z-2y+\delta}\text{N}_{8-z+2y+\gamma}\text{:yEu}^{2+}$	$z$	$y$	$\delta$	
SA3	1	.03	.00	$\text{SiAl}_{0.03}\text{O}_{0.09}\text{N}_{1.00}$	.17	.000	.35	-2.00	.00
SA6	1	.06	.00	$\text{SiAl}_{0.06}\text{O}_{0.18}\text{N}_{1.00}$	.34	.000	.68	-2.00	.00
SA9	1	.09	.00	$\text{SiAl}_{0.09}\text{O}_{0.27}\text{N}_{1.00}$	.50	.000	.99	-2.00	.00
SAE91	1	.09	.01	$\text{SiAl}_{0.09}\text{O}_{0.27}\text{N}_{1.00}\text{Eu}_{0.01}$	.50	.055	1.10	-2.11	.42
SAE93	1	.09	.03	$\text{SiAl}_{0.09}\text{O}_{0.27}\text{N}_{1.00}\text{Eu}_{0.03}$	.50	.165	1.32	-2.33	1.27
SAE95	1	.09	.05	$\text{SiAl}_{0.09}\text{O}_{0.27}\text{N}_{1.00}\text{Eu}_{0.05}$	.50	.275	1.54	-2.55	2.07
SAE97	1	.09	.07	$\text{SiAl}_{0.09}\text{O}_{0.27}\text{N}_{1.00}\text{Eu}_{0.07}$	.50	.385	1.76	-2.77	2.88


**FIGURE 1** Attenuated total reflection infrared (ATR-IR) spectra for as-received perhydropolysilazane (PHPS), Al-modified PHPS (SA9 sample), and Al, Eu-modified PHPS (SAE95 sample): (A) 4000–600  $\text{cm}^{-1}$  and (B) 1240–1080  $\text{cm}^{-1}$ 

As typical results, FTIR spectra of as-received PHPS, Al-modified PHPS, SA9 sample, and Al, Eu-modified PHPS, SAE95 sample are shown in Figure 1A. In addition to characteristic absorption peaks attributed to PHPS at 3400 ( $\nu\text{N-H}$ ), 2152 ( $\nu\text{Si-H}$ ), and 1175 ( $\delta\text{N-H}$ ) and around 832 ( $\nu\text{Si-N-Si}$ )  $\text{cm}^{-1}$ ,<sup>15–20</sup> SA9 sample presented new peaks at 2900 ( $\nu\text{C-H}$ ), 1172 ( $\nu\text{C-C}$ ), 1135 ( $\nu\text{C-O}$ ), and 1118 ( $r\text{CH}_3$ )  $\text{cm}^{-1}$  attributed to  $\text{OCH}(\text{CH}_3)_2$  group<sup>29</sup> originated from  $\text{Al}(\text{OCH}(\text{CH}_3)_2)_3$ ; moreover, the broadband due to  $\nu\text{Si-N-Si}$  showed an apparent red shift (Figure 1B). This peak shift is possibly due to the mass effect on stretching frequencies, that is,  $\text{Al}(\text{OCH}(\text{CH}_3)_2)_3$  reacted with the NH group in PHPS to form N-Al bond,<sup>16</sup> and the substitution of H by the  $\text{Al}(\text{OCH}(\text{CH}_3)_2)_{3-x}$  led to the red shift of the Si-N-Si peak:



On the other hand, the FTIR spectrum of the SAE95 sample was found to be quite similar to that of the SA9 sample.

To study the chemical modification reactions in more details, the reaction of Equation (3) was ex situ monitored by GC-MS analyses. The gas chromatograms and mass spectra recorded for the reference sample, isopropanol and reaction solution for the synthesis of the SA6 sample are given in Figure 2. In this study, a vapor sample was taken from the reaction solution for synthesizing the SA6 sample at RT. In addition to the chromatogram peak I due to the background (mass fragments of the  $m/z$  ratios of 40 and 20 assigned to Ar applied as an inert reaction atmosphere, 32 and 28 due to  $\text{O}_2$  and  $\text{N}_2$ , respectively), isopropanol was identified as peak II by detecting mass fragments at the  $m/z$  ratios of 59 ( $\text{C}_3\text{H}_7\text{O}^+$ ), 45 ( $\text{C}_2\text{H}_5\text{O}^+$ ), 43 ( $\text{C}_3\text{H}_7^+$ ), and 27 ( $\text{C}_2\text{H}_3^+$ )<sup>30</sup> (Figure 2A). On the other hand, the sample vapor evolved at RT exhibited one broad peak (III) around 65.48 s as well as two distinct peaks at 87.88 s (IV) and 90.64 s (V) (Figure 2B). Careful MS analyses for the peak at the retention time of 65.48 s resulted in the detection of the mass fragments attributed to isopropanol as well as those due to the background (Figure 2C), and a single chromatogram peak composed of major fragments at the  $m/z$  ratios of 59 ( $\text{C}_3\text{H}_7\text{O}^+$ ), 45 ( $\text{C}_2\text{H}_5\text{O}^+$ ), 43 ( $\text{C}_3\text{H}_7^+$ ) was extracted from the broad peak III (Figure 2D). On the other hand, the peaks IV and V were identified as xylene used as reaction solvent by detecting typical mass fragments at the  $m/z$  ratios of 106, 91, 77, 65, 51, 39, and 27 and suggested to be assigned to *m*- and *p*-xylene, respectively<sup>30</sup> (Figure 2C). These results clearly revealed that Equation (3) immediately proceeded from RT.

High-temperature reactions during pyrolysis up to 1000°C were further monitored by TG-MS analyses. As typical results, the thermal behaviors of SA9 and SAE95 samples are shown in Figure 3. The TG-curve of the SA9 sample shows two main weight loss regions at RT-150°C (1.25%) and 150–400°C (17.5%), and the total ion

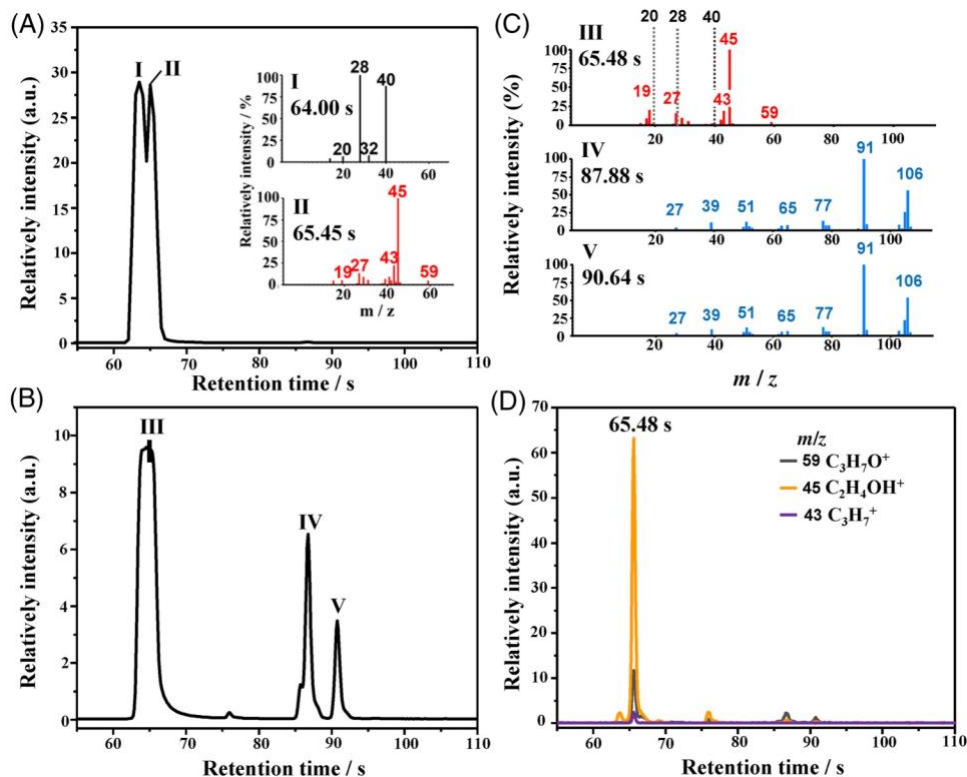


**FIGURE 2** Results of gas chromatography–mass spectrometric (GC–MS) analyses for chemical modification reaction of perhydropolysilazane (PHPS) with  $\text{Al}(\text{OCH}(\text{CH}_3)_2)_3$ . Total ion chromatograms of (A) reference sample, isopropanol and (B) vapor sample taken from reaction solution for synthesis of SA6 sample at room temperature (RT). (C) Mass fragments recorded for each peak shown in (B) and (D) continuous in situ monitoring of gaseous species evolved from reaction solution for synthesis of SA6 sample

current chromatogram (TIC) exhibits two broad peaks centered at 100 and 250°C, respectively (Figure 3A(a)). The mass spectrum measured at 100°C was composed of main fragments at the  $m/z$  ratios of 106, 91, 77, 65, 63, 51, 39, and 27, which are attributed to xylene, whereas those at 133 ( $\text{Si}_3\text{N}_3\text{H}_7^+:\text{N}-\text{SiH}_2-\text{NH}-\text{SiH}_2-\text{NH}-\text{SiH}^+$ ), 75 ( $\text{H}_2\text{SiNHSiH}^{2+}$ ), 45 ( $\text{H}_2\text{SiNH}^+$ ), and 16 ( $\text{NH}^{2+}$ ) are thought to be due to the partial decomposition of low molecular weight fraction of PHPS originally existed or formed in situ via the cleavage of the perhydrosilazane linkages<sup>18</sup> partially proceeded during the chemical modification of PHPS with  $\text{Al}(\text{OCH}(\text{CH}_3)_2)_3$  (Figure 3A(b)). As the molecular ion ( $\text{C}_6\text{H}_4(\text{CH}_3)_2^+$ ,  $m/z = 106$ ) and the tropylium ion ( $\text{C}_7\text{H}_7^+$ ,  $m/z = 91$ ) were only detected up to ~200°C (Figure 3A(c)), the first weight loss from RT to 150°C was due mainly to the residual xylene used as the reaction solvent.

The mass spectrum measured at 250°C (Figure 3A(b)) exhibits three main fragments with  $m/z$  ratios at 41 ( $(\text{CH}_3)_2\text{CH}^+$ ), 29 ( $\text{CH}_3\text{CH}_2^+$ ), and 16 ( $\text{CH}_4^+$ ), which reveals that the second weight loss is attributed to

the thermal decomposition of the residual isopropoxy ( $\text{OCH}_2(\text{CH}_3)_2$ ) group.

The SAE95 sample exhibits similar thermal behavior up to 800°C (Figure 3B(a,b)), and the second weight loss at 150–400°C was 15%, which was also close to that of SA95 (17.5%, Figure 3A(a)). However, this sample presents an additional weight loss at 800–1000°C (5%, Figure 3B(a)). The mass spectrum measured during the third weight loss resulted in the detection of the main gaseous component at the  $m/z$  ratios of 38 and 36 assigned to HCl (Figure 3B(b)).

As shown in Figure 4, the area of the third TIC peak at 800–1000°C was found to be increased with the Eu/Si ratio up to .05 (SAE95 sample) in the *single-source* precursor synthesis at the Al/Si ratio = .09.

Figure 5 shows the thermal behavior under an inert He atmosphere of as-received  $\text{EuCl}_2$ . The TG and DTA curves indicate the gradual weight loss of 16% at 600–1000°C associated with two endothermic peaks at 744 and 852°C. Weight loss was found to be explained by the elimination of one chlorine (Equation 4), Cl (at. wt = 35.45)/ $\text{EuCl}_2$  ( $m_w = 222.86$ )  $\times 100 \approx 16\%$ ), whereas the first endothermic peak at 744°C was found close to the m.p. of  $\text{EuCl}_2$  (738°C<sup>31</sup>).



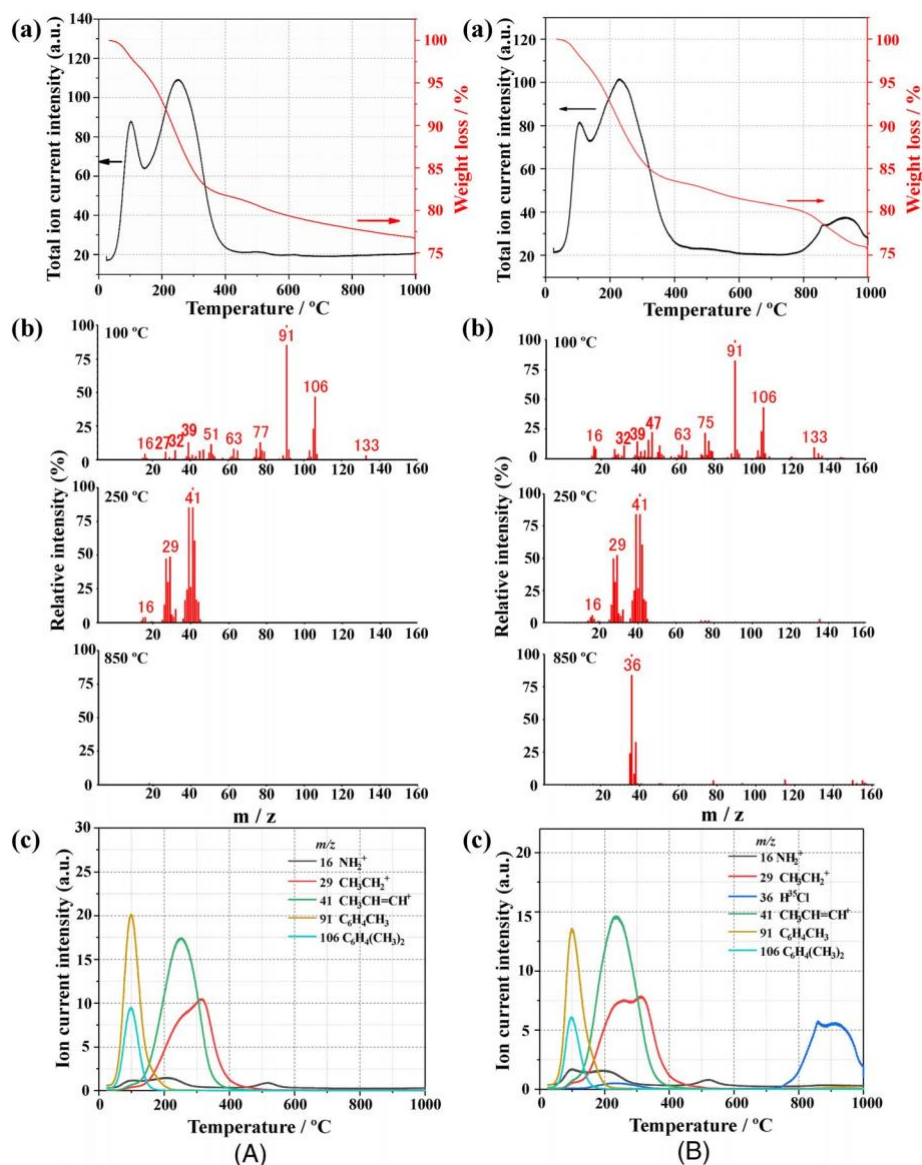


FIGURE 3 Thermal behavior under the flow of Al, (Eu)-modified perhydropolysilazane (PHPS) samples, (A) SA9 and (B) SAE95. (a)

Thermogravimetric (TG) curve and total ion current chromatogram (TICC), (b) mass fragments monitored at specific temperatures of 100, 250, and 850 °C, and (c) selected MS fragments continuously monitored up to 1000 °C

Accordingly, the second endothermic peak at 852 °C was suggested to be ascribed to the melting of the thermally decomposed species such as Eu<sup>+</sup>Cl formed in situ.

These results reveal that the EuCl<sub>2</sub> remained without reacting with the residual alkoxide group, (=N)<sub>m</sub>Al(OR)<sub>3-m</sub> up to ~600 °C, then began to melt accompanied by Cl<sup>-</sup> elimination (Equation 4), which triggered the Eu–N bond formations with silylamino moiety derived from PHPS followed by the elimination of HCl as a byproduct (Equation 5).

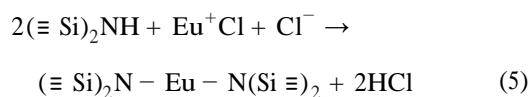


Table 2 shows the chemical compositions of the 1000 °C pyrolyzed samples. The Al/Si and Eu/Si atomic ratios of each sample were slightly higher than the nominal ones, which was due to the volatilization of low molecular weight silicon species as detected by the TG–MS analyses shown in Figure 3.

### 3.2 | Effect of Al content on the formation of polymer-derived β-SiAlON

Figure 6A shows the XRD patterns of the polymer-derived SiAlON samples after the 1800 °C-heat treatment. β-SiAlON (Si<sub>6-z</sub>Al<sub>z</sub>O<sub>z</sub>N<sub>8-z</sub>, z = 2: Si<sub>4</sub>Al<sub>2</sub>O<sub>2</sub>N<sub>6</sub>, JCPDS card

TABLE 2 Chemical compositions of 1000°C as-pyrolyzed samples

Precursor	Pyrolyzed sample	EDS (molar ratio)		Element analysis (wt%)			Empirical formula
		Al/Si	Eu/Si	O	N	C	
SA3	NSA3	.03	.00	3.08	24.92	2.16	SiAl <sub>0.03</sub> O <sub>0.08</sub> N <sub>0.74</sub> C <sub>0.07</sub>
SA6	NSA6	.07	.00	5.43	25.59	2.98	SiAl <sub>0.07</sub> O <sub>0.15</sub> N <sub>0.83</sub> C <sub>0.11</sub>
SA9	NSA9	.11	.00	6.46	21.51	9.46	SiAl <sub>0.11</sub> O <sub>0.26</sub> N <sub>1.03</sub> C <sub>0.38</sub>
SAE91	NSAE91	.11	.02	5.70	22.25	6.25	SiAl <sub>0.11</sub> O <sub>0.19</sub> N <sub>0.84</sub> C <sub>0.28</sub> Eu <sub>0.02</sub>
SAE93	NSAE93	.12	.03	7.60	28.11	5.08	SiAl <sub>0.12</sub> O <sub>0.29</sub> N <sub>1.22</sub> C <sub>0.26</sub> Eu <sub>0.03</sub>
SAE95	NSAE95	.10	.06	7.12	29.00	4.57	SiAl <sub>0.10</sub> O <sub>0.30</sub> N <sub>1.39</sub> C <sub>0.25</sub> Eu <sub>0.06</sub>
SAE97	NSAE97	.13	.08	7.93	26.81	4.61	SiAl <sub>0.13</sub> O <sub>0.36</sub> N <sub>1.38</sub> C <sub>0.27</sub> Eu <sub>0.08</sub>

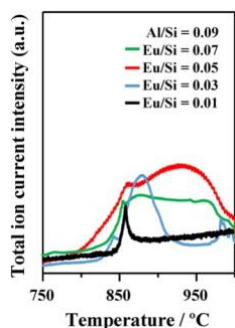


FIGURE 4 The third total ion current chromatogram (TICC) peak at 800–1000°C detected for SAE91 (Eu/Si = .01), SAE93 (Eu/Si = .03), SAE95 (Eu/Si = .05), and SAE97 (Eu/Si = .07) samples synthesized at the Al/Si = .09

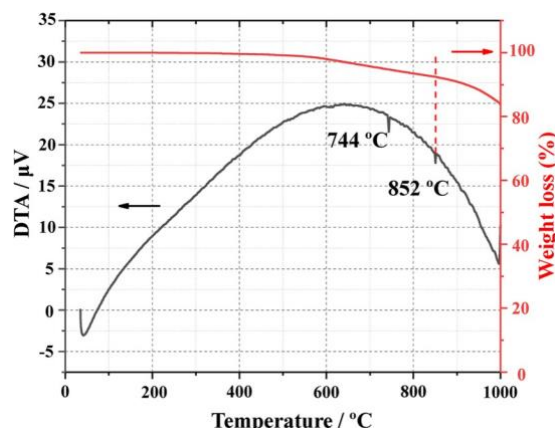


FIGURE 5 Thermogravimetric (TG) and DTA curves of as-received EuCl<sub>2</sub> used in this study

no. 00-048-1616) and  $\alpha$ -SiAlON (Ca<sub>0.8</sub>Si<sub>9.2</sub>Al<sub>2.8</sub>O<sub>1.2</sub>N<sub>14.8</sub>, JCPDS card no. 00-033-0261) are referred to label  $\beta$ - and  $\alpha$ -SiAlON phase. The 1800°C-NSA3 (Al/Si = .03) and

1800°C-NSA6 (Al/Si = .06) samples present a mixture of  $\alpha$ - and  $\beta$ - phases, whereas the 1800°C-NSA9 (Al/Si = .09) sample exhibits  $\beta$ -SiAlON single phase.

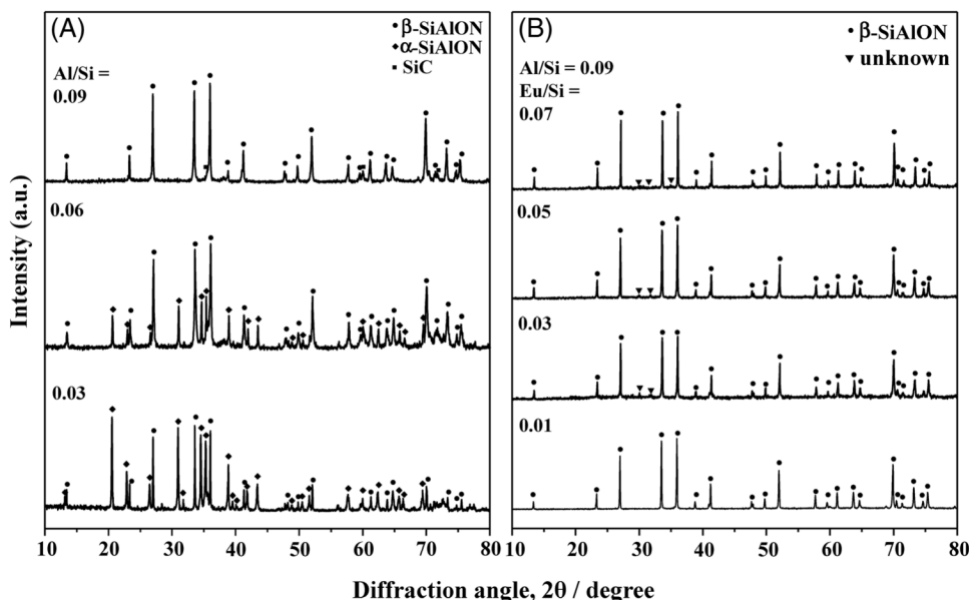


FIGURE 6 X-ray diffraction (XRD) patterns of polymer-derived (A) SiAlON and (B) Eu<sup>2+</sup>-doped SiAlON samples

In our previous studies, the crystallization of  $\alpha$ -Si<sub>3</sub>N<sub>4</sub> from PHPS-derived amorphous silicon nitride (Si–N) was found around 1200°C, and the  $\alpha$ -phase was dominant up to 1800°C,<sup>32</sup> whereas the  $\alpha$ - and  $\beta$ -phase transformation was apparently facilitated in the quaternary Si–M–O–N systems derived from M-modified PHPS to afford  $\beta$ -Si<sub>3</sub>N<sub>4</sub> single phase by the 1800°C heat treatment (M = Y18, Ti<sup>22</sup>).

It is recognized that the transformation between the  $\alpha$  and  $\beta$  phases of Si<sub>3</sub>N<sub>4</sub> has a reconstructive nature,<sup>33,34</sup> which requires significant amounts of thermal energy for the breaking of Si–N bonds.<sup>35–37</sup> Therefore, it is generally suggested that the  $\alpha$ - and  $\beta$ -phase transformation requires a liquid phase, in which  $\alpha$ -Si<sub>3</sub>N<sub>4</sub> grains can dissolve above ~1400°C to assist the necessary atomic diffusion for promoting the  $\alpha$ -/ $\beta$ -phase transformation.<sup>33,36–38</sup>

In the case of the quaternary SiAlON system, the aluminum–silicon oxynitride liquid phase was suggested to be formed in situ,<sup>39</sup> which could promote the  $\alpha$ -/ $\beta$ -phase transformation by analogy with the transformation from  $\alpha$ - to  $\beta$ -Si<sub>3</sub>N<sub>4</sub> above 1400°C and the subsequent solid solution formation to afford stoichiometric  $\beta$ -SiAlON (Si<sub>6-z</sub>Al<sub>z</sub>O<sub>z</sub>N<sub>8-z</sub> (0 ≤ z ≤ 4.2)).<sup>39</sup>

Accordingly, an in situ formation of  $\beta$ -SiAlON from the present *single-source* precursor-derived amorphous compound is suggested to proceed by the nucleation and crystallization of  $\alpha$ -Si<sub>3</sub>N<sub>4</sub> or  $\alpha$ -SiAlON and subsequent  $\alpha$ -/ $\beta$ -phase transformation via the dissolution, diffusion, and re-precipitation processes through the transient liquid phase formed in situ. The amount of the transient liquid phase increased consistently with the Al and O contents, that is, the Al/Si ratio in the *single-source* precursor synthesis, and the resulting  $\beta$ -phase content defined as the  $\beta/(\beta + \alpha)$  phase ratio (Equation 1) of the 1800°C-heat samples was found to increase consistently with the Al/Si ratio (Tables 2 and 3). These results reveal that the Al/Si ratio of .09 is required for the  $\beta$ -SiAlON single-phase formation through the PDCs route investigated in this study. However, the amount of carbon impurity in the 1800°C-NSA9 sample was 6.87 wt% (Table 3), which was due to the formation of the secondary phase assigned to  $\beta$ -silicon carbide ( $\beta$ -SiC, JCPDS card 01-073-1665, Figure 6A).

### 3.3 | Effect of Eu<sup>2+</sup> concentration on the formation and properties of polymer-derived $\beta$ -SiAlON:Eu<sup>2+</sup> phosphors

XRD patterns of the Eu<sup>2+</sup>-doped samples are shown in Figure 6B. Regardless of the Eu/Si ratio in the *single-source* precursor synthesis at the Al/Si = .09, the  $\beta$ -SiC formation was successfully suppressed, and all the samples exhibited  $\beta$ -SiAlON single phase. However, at the Eu/Si ratios of .03–.07, an unknown minor impurity phase appeared,

TABLE 3 Chemical compositions of 1800°C-heated

	EDS (molar ratio)		Element analysis (wt%)		Chemical composition			
	Eu <sup>2+</sup>	Si	wt%	at%	Si <sub>6-z</sub> Al <sub>z</sub> O <sub>z</sub> N <sub>8-z+2y+y</sub> :yEu <sup>2+</sup>	Eu <sup>2+</sup> (at%)	$\beta$ -phase content (%)	
1800°C-	.03	.00	2.06	34.32	1.57	SiAl <sub>0.03</sub> O <sub>0.06</sub> N <sub>1.12</sub> C <sub>0.01</sub>	.00	51.1
1800°C-	.07	.00	2.03	34.75	1.58	SiAl <sub>0.07</sub> O <sub>0.06</sub> N <sub>1.21</sub> C <sub>0.06</sub>	.00	67
NSA9	.10	.00	4.02	31.44	6.87	SiAl <sub>0.10</sub> O <sub>0.13</sub> N <sub>1.20</sub> C <sub>0.31</sub>	.00	100
1800°C-	.10	.01	2.33	34.37	1.80	SiAl <sub>0.10</sub> O <sub>0.07</sub> N <sub>1.28</sub> C <sub>0.08</sub> Eu <sub>0.01</sub>	.41	100
NSA9C-	.10	.03	2.22	34.54	.77	SiAl <sub>0.10</sub> O <sub>0.08</sub> N <sub>1.35</sub> C <sub>0.04</sub> Eu <sub>0.03</sub>	1.15	100
1800°C-	.10	.04	2.83	34.93	.13	SiAl <sub>0.10</sub> O <sub>0.10</sub> N <sub>1.47</sub> C <sub>0.01</sub> Eu <sub>0.04</sub>	1.48	100
NSA9C-	.11	.06	1.86	35.17	.16	SiAl <sub>0.11</sub> O <sub>0.07</sub> N <sub>1.60</sub> C <sub>0.01</sub> Eu <sub>0.06</sub>	2.11	100

<sup>a</sup>The z value was calculated as  $\beta$ -SiAlON single phase.

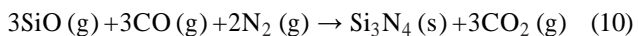
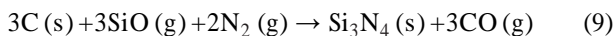
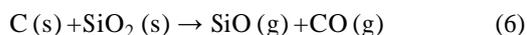
<sup>b</sup> $\beta$ -SiC formed as a minor secondary phase.

Abbreviation: EDS, energy-dispersive X-ray spectrometer.

and its diffraction pattern (marked by ▼) was found to be similar to the U phase of SiAlON reported for the intergranular crystalline phase of rare-earth (Re)-doped SiAlON polycrystallites (Re = La, Nd).<sup>40,41</sup>

The chemical compositions of all the samples after the 1800°C-heat treatment were listed in Table 3. The  $z$  and  $y$  values were calculated by the modified formula of  $\text{Si}_{6-z}\text{Al}_z\text{O}_{z-2y+\delta}\text{N}_{8-z+2y+\gamma}:\text{yEu}^{2+}$ . The carbon impurity content was significantly decreased by the doping of  $\text{Eu}^{2+}$ : The carbon content decreased from 6.87 to 1.80 wt% at the  $\text{Eu}^{2+}$ -doping of .41 at% (1800°C-NSAE91 sample) and further decreased to .13 (1800°C-NSAE95 sample) and .16 wt% (1800°C-NSAE97 sample) at the  $\text{Eu}^{2+}$ -doping of 1.48 and 2.11 at%, respectively. On the other hand, the N/Si ratio, that is, the nitrogen content of the 1800°C-heated samples increased with increasing the amount of  $\text{Eu}^{2+}$ -doping.

During the heat treatment up to 1800°C for 1 h, alongside the in situ  $\beta$ -SiAlON formation, carbothermal reduction of silica ( $\text{SiO}_2$ ) species (Equations 6–8) and subsequent nitridation reactions (Equations 9–10) proceeded as reported for  $\text{SiO}_2$  in the presence of free carbon.<sup>42</sup> The results obtained in this study strongly suggest that these reactions in the polymer-derived amorphous compound were facilitated consistently with the amount of  $\text{Eu}^{2+}$ -doping, which avoided the formation of SiC phase (Equation 11).



Loehmann reported that the glass transition temperature ( $T_g$ ) of the series of Y–Si–Al–O–N glasses varied from ~810 to 920°C and suggested that the  $T_g$  increased consistently with the nitrogen content in the range of 1.5–7 at%.<sup>43</sup> Pomeroy and Hampshire<sup>44,45</sup> also examined the properties of various metal cation-doped SiAlON and SiMgON glasses and suggested that, in addition to the  $T_g$ , the Littleton softening temperatures<sup>46</sup> and the dilatometric softening temperatures also increase linearly with nitrogen content in the range of 0–8 at%,<sup>45</sup> whereas the viscosity of these glasses measured at 875–930°C depends not only

on the nitrogen content but also varies significantly by the type and amount of the dopant cation.<sup>45</sup>

As shown in Table 2, the nitrogen content of the 1000°C-pyrolyzed samples increased with the amount of the  $\text{Eu}^{2+}$ -doping. Accordingly, it is difficult to expect that the formation onset temperature of the transient liquid phase decreases consistently with the amount of  $\text{Eu}^{2+}$ -doping. To clarify the dominant mechanism, further investigations are necessary; however, one possible suggestion is the significant decrease in the viscosity of the transient liquid phase by the  $\text{Eu}^{2+}$ -doping, which accelerates the initial solid-state carbothermal reduction (Equation 6), and then subsequent reactions (Equations 7 and 8) to release gaseous species such as  $\text{CO}_2$  and CO followed by nitridation reactions (Equations 10 and 11) to afford the  $\text{Eu}^{2+}$ -doped  $\beta$ -SiAlON with the chemical composition close to the theoretical one expressed as  $\text{Si}_{6-z}\text{Al}_z\text{O}_{z-2y}\text{N}_{8-z+2y}:\text{yEu}^{2+}$ .

As a typical microstructure observation result, SEM images of 1800°C-NSAE91 sample ( $z = .55$ ,  $\text{Eu}^{2+}$  .41 at%) and 1800°C-NSAE95 sample ( $z = .55$ ,  $\text{Eu}^{2+}$  1.48 at%) are shown in Figure 7. All of the polymer-derived  $\beta$ -SiAlON: $\text{Eu}^{2+}$  samples exhibited typical rod-like  $\beta$ -SiAlON grains, and it was found that the increase in the  $\text{Eu}^{2+}$  concentration did not affect the morphology of the matrix  $\beta$ -SiAlON.

However, as shown in Figure 8, some equiaxed grains embedded within the rod-like  $\beta$ -SiAlON grains were observed for the 1800°C-NSAE97 sample, and the morphology was quite similar to those previously reported for the SiAlON polytypoid phases such as 12H and 15R.<sup>47</sup> These Al-rich polytypoid phases were found to be formed in the case of excess  $\text{Eu}^{2+}$  concentration in the  $\text{Eu}^{2+}$ -doped SiAlON ceramics.<sup>6</sup> In addition to the unknown phase formation (Figure 6B), phase purity of the host  $\beta$ -SiAlON was suggested to be decreased due to the 2.11 at%  $\text{Eu}^{2+}$ -doping.

The RT PL excitation and emission spectra of the polymer-derived  $\beta$ -SiAlON: $\text{Eu}^{2+}$  phosphor samples are shown in Figure 9. The excitation spectra (Figure 9A) were monitored at the appropriate maximum emission wavelengths of each sample shown in Figure 9B. The emission spectra shown in Figure 9B,C were monitored under excitation at 410 and 460 nm, respectively. All the samples except the 1800°C-NSAE97 sample show a similar shape of excitation spectrum with a dominant broad peak around 290 to 300 nm and several peaks at around 410 to 500 nm attributed to the absorptions of the host lattice and the  $4f^7-4f^65d^1$  transitions of dopant  $\text{Eu}^{2+}$  cations, respectively.<sup>6</sup> These polymer-derived  $\beta$ -SiAlON: $\text{Eu}^{2+}$  phosphor samples exhibit a typical green emission under violet light excitation ( $\lambda_{\text{ex}} = 410$  nm, Figure 9B) or blue light excitation ( $\lambda_{\text{ex}} = 460$  nm, Figure 9C). Moreover, the green emission intensity was found to increase consistently

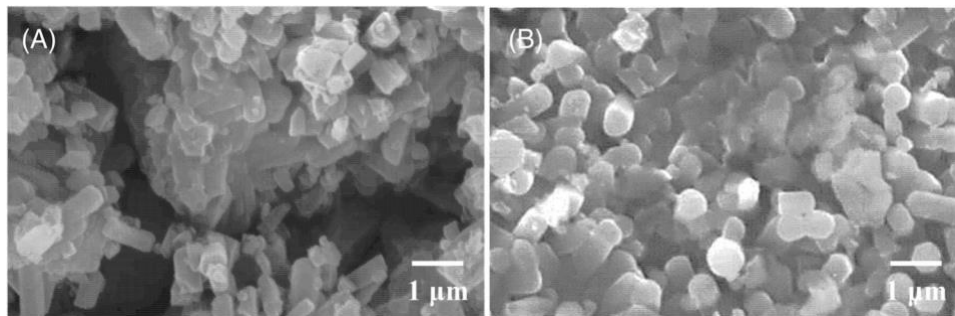


**FIGURE 7** Scanning electron microscope (SEM) images showing morphology of (A) 1800°C-NSAE91 sample and (B) 1800°C-NSAE95 sample

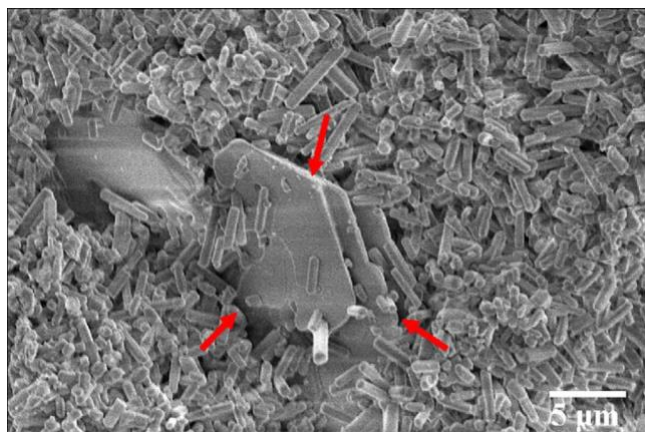


**FIGURE 8** Scanning electron microscope (SEM) image of 1800°C-NSAE97 sample showing an equiaxed grain (marked by red arrows) embedded within  $\beta$ -SiAlON rod-like grains

with  $\text{Eu}^{2+}$  concentration from .41 (1800°C-NSAE91 sample) to 1.48 at% (1800°C-NSAE95 sample). As shown in Figure 7, the 1800°C-NSAE95 sample was composed of

fine-grained polycrystallites similar to those of the 1800°C-NSAE91 sample, whereas the green emission intensity of the 1800°C-NSAE95 sample was found to be approximately two times higher than that of the 1800°C-NSAE91 sample (Figure 9B,C).

On the other hand, the 1800°C-NSAE97 sample ( $z = .59$ ,  $\text{Eu}^{2+}$  2.11 at%) showed an apparent decrease in the green emission intensity and exhibited an additional weak broad peak centered around 450 nm, which reveals the different surrounding environment of  $\text{Eu}^{2+}$  cations. As discussed earlier, the formation of impurity phases, such as U-phase and SiAlON polytypoid phases, were suggested for the 1800°C-NSAE97 sample, and excess  $\text{Eu}^{2+}$  cations in this sample were thought to be located in these impurity phases with lower crystal field strength, which led to the blue shift of the green emission peak due to the weaker split of the 5d energy level of  $\text{Eu}^{2+}$  ions.

In terms of the green emission intensity, the critical  $\text{Eu}^{2+}$  concentration of the polymer-derived host  $\beta$ -SiAlON with  $z = .55$  was found to be governed by the impurity phase formation prior to the concentration quenching. However,

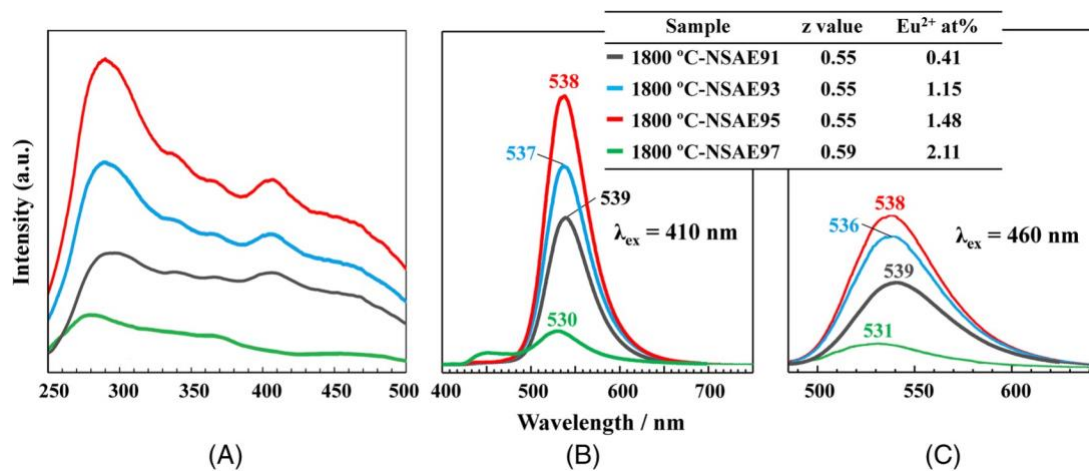


**FIGURE 9** (A) Excitation and (B), (C) emission spectra of polymer-derived  $\beta$ -SiAlON: $\text{Eu}^{2+}$  phosphor samples measured at room temperature (RT)

the green emission intensity was successfully enhanced by the  $\text{Eu}^{2+}$ -doping up to 1.48 at%, and this value was approximately three times higher than that (.5 at%) previously suggested for the  $\text{Eu}^{2+}$ -activated  $\beta$ -SiAlON with  $z = .5$  fabricated by the conventional powder metallurgy method. These results suggest that the PDCs route investigated in this study offers some potential benefits for developing high-performance  $\beta$ -SiAlON: $\text{Eu}^{2+}$  green phosphors such as higher critical  $\text{Eu}^{2+}$  concentration up to approximately 1.5 mol% for the host  $\beta$ -SiAlON ( $z = .55$ ), and the host grain refinement easy for assembling w-LEDs without intensive pulverization process.

## 4 | CONCLUSIONS

In this work,  $\beta$ -SiAlON: $\text{Eu}^{2+}$  phosphors were synthesized from *single-source* precursors, chemically modified PHPS with  $\text{Al}(\text{OCH}(\text{CH}_3)_2)_3$ , and  $\text{EuCl}_2$ . The chemical modification reactions were intensively studied by a set of characterization techniques, including IR spectroscopy, ex situ reaction monitoring by GC-MS analyses up to  $140^\circ\text{C}$ , and in situ thermal behavior analysis up to  $1000^\circ\text{C}$  of the *single-source* precursors by TG-MS analyses. The *single source* precursors were successfully converted to  $\beta$ -SiAlON: $\text{Eu}^{2+}$  phosphors by  $1000^\circ\text{C}$ -pyrolysis in  $\text{N}_2$  and subsequent  $1800^\circ\text{C}$ -heat treatment for 1 h under an  $\text{N}_2$  gas pressure at 980 kPa. The relationships between the amount of  $\text{Eu}^{2+}$ -doping, phase purity, grain growth and morphology of host  $\beta$ -SiAlON, and PL properties were discussed. The results can be summarized as follows:

- (1)  $\text{Al}(\text{OCH}(\text{CH}_3)_2)_3$  reacted with PHPS immediately at RT, whereas  $\text{EuCl}_2$  remained during the precursor synthesis in refluxing xylene at  $140^\circ\text{C}$ .
- (2) At around  $744^\circ\text{C}$ , the  $\text{EuCl}_2$  began to melt accompanied by  $\text{Cl}^-$  elimination, which triggered Eu-N bond formations with silylamino moiety derived from PHPS associated with the elimination of HCl up to  $1000^\circ\text{C}$ .
- (3) The (Al + Eu)/Si atomic ratio of around .14 was found as critical for the chemical modification of PHPS via N-M (M = Al or Eu) bond formations to afford single-phase  $\beta$ -SiAlON: $\text{Eu}^{2+}$  phosphor with a chemical composition close to the theoretical one expressed by the formula,  $\text{Si}_{6-z}\text{Al}_z\text{O}_{z-2y}\text{N}_{8-z+2y} : y\text{Eu}^{2+}$ .
- (4) The critical  $\text{Eu}^{2+}$  concentration in the present polymer-derived  $\beta$ -SiAlON: $\text{Eu}^{2+}$  with  $z = .55$  was suggested as high as 1.48 at%.
- (5) The Eu-N bond performed in the polymer-derived multicomponent amorphous compound might act an important role in the enhanced critical  $\text{Eu}^{2+}$  concentration in the polymer-derived host  $\beta$ -SiAlON formed in situ.

- (6) The polymer-derived host  $\beta$ -SiAlON ( $z = .55$ ) kept the fine-gained polycrystallites with rod-like morphology at the  $\text{Eu}^{2+}$ -doping up to 1.48 at%, whereas the green emission intensity under violet or blue light excitation increased consistently with the amount of  $\text{Eu}^{2+}$ -doping and reached the highest at the suggested critical concentration of 1.48 at%.

## ACKNOWLEDGMENTS

This work was supported by the Japan Science and Technology Agency (JST) SPRING, Grant no. JPMJSP 2112. Dr. Samuel Bernard, Dr. Philippe Thomas, and Prof. Yuji Iwamoto would like to thank CNRS who financially supported the present work via the International Research Project (IRP) "Ceramics materials for societal challenges."

## AUTHOR CONTRIBUTIONS

Yang Gao conceived and planned this study, and drafted the manuscript; Yang Gao, Ryo Iwasaki, Daiki Hamana, Junya Iihama, and Munni Kumari contributed to the evaluation of samples; Sawao Honda and Tomokatsu Hayakawa contributed to Formal analysis; Philippe Thomas and Samuel Bernard reviewed the draft; Yuji Iwamoto conceived, reviewed, and supervised this work. All authors have read and agreed to the published version of the manuscript.

## ORCID

Sawao Honda  <https://orcid.org/0000-0002-5760-5014>

Samuel Bernard  <https://orcid.org/0000-0001-5865-0047>

Yuji Iwamoto  <https://orcid.org/0000-0002-6927-5446>

## REFERENCES

1. Wang L, Xie RJ, Suehiro T, Takeda T, Hirotsuki N. Down-conversion nitride materials for solid state lighting: recent advances and perspectives. *Chem Rev.* 2008;118(2):1951–2009. <https://doi.org/10.1021/acs.chemrev.7b00284>
2. Wang ZB, Ye W, Chu IH, Ong SP. Elucidating structure–composition–property relationships of the  $\beta$ -SiAlON: $\text{Eu}^{2+}$  phosphor. *Chem Mater.* 2016;28(23):8622–30. <https://doi.org/10.1021/acs.chemmater.6b03555>
3. Takahashi K, Xie RJ, Hirotsuki N. Toward higher color purity and narrower emission band  $\beta$ -sialon: $\text{Eu}^{2+}$  by reducing the oxygen concentration. *ECS Solid State Lett.* 2011;14(11):E38–40. <https://doi.org/10.1149/2.017111esl>
4. Li S, Wang L, Tang DM, Cho YJ, Liu XJ, Zhou XT, et al. Achieving high quantum efficiency narrow-band  $\beta$ -sialon: $\text{Eu}^{2+}$  phosphors for high-brightness LCD backlights by reducing the  $\text{Eu}^{3+}$  luminescence killer. *Chem Mater.* 2018;30(2):494–505. <https://doi.org/10.1021/acs.chemmater.7b04605>
5. Zhu XW, Masubuchi Y, Motohashi T, Kikkawa S. The z value dependence of photoluminescence in  $\text{Eu}^{2+}$ -doped  $\beta$ -SiAlON

- ( $\text{Si}_{6-z}\text{Al}_z\text{O}_z\text{N}_{8-z}$ ) with  $1 \leq z \leq 4$ . *J Alloys Compd.* 2010;489(1):157–61. <https://doi.org/10.1016/j.jallcom.2009.09.042>
6. Xie RJ, Hirosaki N, Li HL, Li YQ, Mitomo M. Synthesis and photoluminescence properties of  $\beta$ -sialon: $\text{Eu}^{2+}$  ( $\text{Si}_{6-z}\text{Al}_z\text{O}_z\text{N}_{8-z}$ : $\text{Eu}^{2+}$ ): a promising green oxynitride phosphor for white light-emitting diodes. *J Electrochem Soc.* 2007;154(10):J314–9. <https://doi.org/10.1149/1.2768289>
  7. Kroke E, Li YL, Konetschny C, Lecomte E, Fasel C, Riedel R. Silazane derived ceramics and related materials. *Mater Sci Eng R Rep.* 2000;26(4–6):97–199. [https://doi.org/10.1016/S0927-796X\(00\)00008-5](https://doi.org/10.1016/S0927-796X(00)00008-5)
  8. Colombo P, Mera G, Riedel R, Soraru GD. Polymer-derived ceramics: 40 years of research and innovation in advanced ceramics. *J Am Ceram Soc.* 2010;93(7):1805–1837. <https://doi.org/10.1111/j.1551-2916.2010.03876.x>
  9. Ionescu E, Kleebe HJ, Riedel R. Silicon-containing polymer-derived ceramic nanocomposites (PDC-NCs): preparative approaches and properties. *Chem Soc Rev.* 2012;41(15):5032–52. <https://doi.org/10.1039/C2CS15319J>
  10. Iwamoto Y, Ionescu E, Bernard S. Pre-ceramic polymers as precursors of advanced ceramics: the polymer-derived ceramics (PDCs) route. In: Hampshire S, Leriche A, editors. *Encyclopedia of materials: technical ceramics and glasses.* Amsterdam: Elsevier; 2021.
  11. Sanchez C, Boissiere C, Cassaignon S, Chanéac C, Durupthy O, Faustini M, et al. Molecular engineering of functional inorganic and hybrid materials. *Chem Mater.* 2014;26(1):221–38. <https://doi.org/10.1021/cm402528b>
  12. Clément S, Mehdi A. Sol-gel chemistry: from molecule to functional materials. *Molecules.* 2020;25(11):2538. <https://doi.org/10.3390/molecules25112538>
  13. Sanchez C, Rozes L, Ribot F, Laberty-Robert C, Grosso D, Sassoie C, et al. “Chimie douce”: a land of opportunities for the designed construction of functional inorganic and hybrid organic-inorganic nanomaterials. *C R Chim.* 2010;13(1–2):3–39. <https://doi.org/10.1016/j.crci.2009.06.001>
  14. Lale A, Schmidt M, Mallmann MD, Bezerra AVA, Acosta ED, Machado RAF, et al. Polymer-derived ceramics with engineered mesoporosity: from design to application in catalysis. *Surf Coat Technol.* 2018;350(25):569–86. <https://doi.org/10.1016/j.surfcoat.2018.07.061>
  15. Funayama O, Kato T, Tashiro Y, Isoda T. Synthesis of a polyborosilazane and its conversion into inorganic compounds. *J Am Ceram Soc.* 1993;76(3):717–23. <https://doi.org/10.1111/j.1151-2916.1993.tb03665.x>
  16. Funayama O, Tashiro Y, Aoki T, Isoda T. Synthesis and pyrolysis of polyaluminosilazane. *J Ceram Soc Jpn.* 1994;102(1190):908–12. <https://doi.org/10.2109/jcersj.102.908>
  17. Iwamoto Y, Matsubara H, Brook RJ. Microstructural development of  $\text{Si}_3\text{N}_4$  ceramics derived from polymer precursors. *Ceram Trans.* 1995;51:193–7.
  18. Iwamoto Y, Kikuta K, Hirano S. Microstructural development of  $\text{Si}_3\text{N}_4$ - $\text{SiC}$ - $\text{Y}_2\text{O}_3$  ceramics derived from polymeric precursors. *J Mater Res.* 1998;13(2):353–61. <https://doi.org/10.1557/JMR.1998.0047>
  19. Iwamoto Y, Kikuta K, Hirano S.  $\text{Si}_3\text{N}_4$ - $\text{SiC}$ - $\text{Y}_2\text{O}_3$  ceramics derived from yttrium-modified block copolymer of perhydropolysilazane and hydroxy-polycarbosilane. *J Mater Res.* 1999;14(5):1886–95. <https://doi.org/10.1557/JMR.1999.0253>
  20. Iwamoto Y, Kikuta K, Hirano S.  $\text{Si}_3\text{N}_4$ - $\text{TiN}$ - $\text{Y}_2\text{O}_3$  ceramics derived from chemically modified perhydropolysilazane. *J Mater Res.* 1999;14(11):4294–301. <https://doi.org/10.1557/JMR.1999.0582>
  21. Tada S, Mallmann MD, Takagi H, Iihama J, Asakuma N, Asaka T, et al. Low temperature in situ formation of cobalt in silicon nitride toward functional nitride nanocomposites. *Chem Commun.* 2021;16:2057–60. <https://doi.org/10.1039/D0CC07366K>
  22. Iwamoto Y, Kikuta K, Hirano S. Synthesis of polytitanosilazanes and conversion into  $\text{Si}_3\text{N}_4$ - $\text{TiN}$  ceramics. *J Ceram Soc Jpn.* 2000;108(4):350–6. [https://doi.org/10.2109/jcersj.108.1256\\_350](https://doi.org/10.2109/jcersj.108.1256_350)
  23. Iwamoto Y, Kikuta K, Hirano S. Crystallization and microstructure development of  $\text{Si}_3\text{N}_4$ - $\text{Ti(C, N)}$ - $\text{Y}_2\text{O}_3$  ceramics derived from chemically modified perhydropolysilazane. *J Ceram Soc Jpn.* 2000;108(1264):1072–8. [https://doi.org/10.2109/jcersj.108.1264\\_1072](https://doi.org/10.2109/jcersj.108.1264_1072)
  24. Lale A, Mallmann MD, Tada S, Bruma A, Özkaz S, Kumar R, et al. Highly active, robust and reusable micro-/mesoporous  $\text{TiN/Si}_3\text{N}_4$  nanocomposite-based catalysts for clean energy: understanding the key role of  $\text{TiN}$  nanoclusters and amorphous  $\text{Si}_3\text{N}_4$  matrix in the performance of the catalyst system. *Appl Catal B.* 2020;272(5):118975. <https://doi.org/10.1016/j.apcatb.2020.118975>
  25. Soraru GD, Ravagni A, Campostrini R, Babonneau F. Synthesis and characterization of  $\beta'$ - $\text{SiAlON}$  ceramics from organosilicon polymers. *J Am Ceram Soc.* 1991;74(9):2220–3. <https://doi.org/10.1111/j.1151-2916.1991.tb08288.x>
  26. Bernardo E, Colombo P, Hampshire S.  $\text{SiAlON}$ -based ceramics from filled preceramic polymers. *J Am Ceram Soc.* 2006;89(12):3839–42. <https://doi.org/10.1111/j.1551-2916.2006.01287.x>
  27. Parciannello G, Bernardo E, Colombo P. Optimization of phase purity of  $\beta'$ -sialon ceramics produced from silazanes and nanosized alumina. *J Am Ceram Soc.* 2012;95(7):2148–54. <https://doi.org/10.1111/j.1551-2916.2012.05179.x>
  28. Gazzara CP, Messier DR. Determination of phase content of  $\text{Si}_3\text{N}_4$  by X-ray diffraction analysis. *Ceram Bull.* 1977;56(9):777–80. <https://bulletin-archive.ceramics.org/1977-09/>
  29. Christensen PA, Mashhadani ZTAW, Md Ali AHB, Carroll MA, Philip Martin PA. The production of methane, acetone, “cold” CO and oxygenated species from isopropyl alcohol in a non-thermal plasma: an in-situ FTIR study. *J Phys Chem A.* 2018;122(17):4273–84. <https://doi.org/10.1021/acs.jpca.7b12297>
  30. National Institute of Standards (NIST) Chemistry WebBook, SRD 69, 2022. <http://webbook.nist.gov>
  31. Polyachenok OG, Novikov GI. Saturated vapor pressures of  $\text{SmCl}_2$ ,  $\text{EuCl}_2$ ,  $\text{YbCl}_2$ . *Zh Neorg Khim.* 1963;8:2631–4. ISSN 0044–457X
  32. Iwamoto Y, Völger W, Kroke E, Riedel R, Saitou T, Matsunaga K. Crystallization behavior of amorphous silicon carbonitride ceramics derived from organometallic precursors. *J Am Ceram Soc.* 2001;84:2170–8. <https://doi.org/10.1111/j.1151-2916.2001.tb00983.x>
  33. Cao G, Metselaar R.  $\alpha'$ -Sialon ceramics: a review. *Chem Mater.* 1991;3(2):242–52. <https://doi.org/10.1021/cm00014a009>
  34. Hampshire S, Park HK, Thompson DP, Jack KH.  $\alpha$ -Sialon ceramics. *Nature.* 1978;274:880–2. <https://doi.org/10.1038/274880a0>

35. Weiss J. Silicon nitride ceramics: composition, fabrication parameters, and properties. *Annu Rev Mater Sci.* 1981;11:381–9. <https://doi.org/10.1146/annurev.ms.11.080181.002121>
36. Messier DR, Riley FL, Brook RJ. The  $\alpha/\beta$  silicon nitride phase transformation. *J Mater Sci.* 1978;13:1199–205. <https://doi.org/10.1007/BF00544725>
37. Jack KH. Chapter V – The relationship of phase diagrams to research and development of sialons. In: Alper AM, editor. *Phase diagrams; materials science and technology.* vol. V. New York: Academic Press; 1978. p. 241–5. <https://doi.org/10.1016/B978-0-12-053205-6.X5001-3>
38. Izhevskiy VA, Genova LA, Bressiani JC, Aldinger F. Progress in SiAlON ceramics. *J Eur Ceram Soc.* 2000;20(13):2275–95. [https://doi.org/10.1016/S0955-2219\(00\)00039-X](https://doi.org/10.1016/S0955-2219(00)00039-X)
39. Zhou Y, Yoshizawa Y, Hirao K, Lenčič Z, Šajgalik P. Preparation of Eu-doped  $\beta$ -SiAlON phosphors by combustion synthesis. *J Am Ceram Soc.* 2008;91(9):3082–5. <https://doi.org/10.1111/j.1551-2916.2008.02531.x>
40. Käll PO, Grins J, Olsson PO, Liddell K, Korgul P, Thompson DP. Preparation and crystal structure of U-phase  $\text{Ln}_3(\text{Si}_{3-x}\text{Al}_{3+x})\text{O}_{12+x}\text{N}_{2-x}$  ( $x \approx 0.5$ , Ln = La, Nd). *J Mater Chem.* 1991;1(2):239–44. <https://doi.org/10.1039/JM9910100239>
41. Huang S, Huang Z, Liu YG, Fang M, Yin L, Huang J. Microstructural and mechanical characterization of pressure-less sintered AlN-polytypoid based composites by compositional design. *J Am Ceram Soc.* 2012;95(6):2044–50. <https://doi.org/10.1111/j.1551-2916.2012.05176.x>
42. Weimer AW, Eisman GA, Sunsnitzky DW, Beaman DR, McCoy JW. Mechanism and kinetics of the carbothermal nitridation synthesis of  $\alpha$ -silicon nitride. *J Am Ceram Soc.* 1997;80(11):2853–63. <https://doi.org/10.1111/j.1151-2916.1997.tb03203.x>
43. Lehman RE. Preparation and properties of yttrium-silicon-aluminum oxynitride glasses. *J Am Ceram Soc.* 1979;62(9–10):491–3. <https://doi.org/10.1111/j.1151-2916.1979.tb19113.x>
44. Hampshire S. Oxynitride glasses. In: Mahajan S, Buschow KHJ, Cahn R, Flemings MC, Ilschner B, Kramer EJ, et al, editors. *Encyclopedia of materials: science and technology.* Oxford: Pergamon; 2001. p. 1–7.
45. Pomeroy MJ, Hampshire S. SiAlON glasses: effects of nitrogen on structure and properties. *J Ceram Soc Jpn.* 2008;116(6):755–61. <https://doi.org/10.2109/jcersj2.116.755>
46. Lofaj F, Satet R, Hoffmann MJ, de Arellano López AR. Thermal expansion and glass transition temperature of the rare-earth doped oxynitride glasses. *J Eur Ceram Soc.* 2004;24:3377–85. <https://doi.org/10.1016/j.jeurceramsoc.2003.10.012>
47. Hou X, Yue C, Guo M, Wang X, Zhang M, Chou KC. Synthesis, phase transformation and mechanical property of SiAlON ceramics from coal gangue. *J Min Metall A.* 2014;50(1):47–55. <https://doi.org/10.5937/JMMA1401047H>